

Plasmonic Resonance Effects for Tandem Receiving-Transmitting Nanoantennas

Pavel Ginzburg,^{*,†} Amir Nevet,[†] Nikolai Berkovitch,[†] Alexander Normatov,[†] Gilad M. Lerman,[†] Avner Yanai,[†] Uriel Levy,[†] and Meir Orenstein[†]

[†]EE department, Technion—Israel Institute of Technology, Technion City, Haifa 32000, Israel, and [†]Department of Applied Physics, The Benin School of Engineering and Computer Science, The Center for Nanoscience and Nanotechnology, The Hebrew University of Jerusalem, Jerusalem, 91904, Israel

ABSTRACT A nanoplasmonic “transceiver” was assembled to examine the efficiency of coupled plasmonic antennas and their resonance interactions. In particular, plasmonic focusing receiver antenna coupled to transmitting annular antenna having a short central plasmonic wire was measured. The receiver collected incoming radially polarized light and efficiently focused and coupled it to a rear side transmitter comprised of a short resonant plasmonic wire and annular aperture. Transmission spectra exhibited a substantial signature of the wire Fabry–Perot resonances. The wire antenna crosssection was improved by nearly 3 orders of magnitude by the focusing antenna system.

KEYWORDS Plasmonics, nanoantenna, field enhancement, unidirectional operation, nanoparticles, nanolithography

There is an increasing interest in the manipulation of light-matter interaction on the nanoscale, promising a large variety of applications. The significant progress in this field is enabled by the fast development in nanometer processing techniques, such as electron-beam and ion-beam lithography, allowing fabrication of high quality metal nanostructures.¹

To cause an efficient interaction with light on the nanoscale, one has to confine the electromagnetic field much beyond its free-space wavelength. While conventional dielectric structures are incapable of supporting optical fields much below a half-wavelength cube volume, metallic structures at visible and near-infrared (NIR) regimes, having negative electrical-permittivity, do not exhibit such a limitation.² Metal substances may support unique modes called surface plasmons polaritons (SPPs)^{3,4} which may be guided by waveguides⁵ or localized by either single nanometric particles^{6,7} or coupled nanometric particles⁸ in the subwavelength regime. Efficient focusing of SPPs is significant for nanoscale interactions and it was proposed and demonstrated in a variety of configurations, such as adiabatic conical metal rod,⁹ and tapered^{10–12} or abrupt impedance matched metal/insulator/metal (MIM) plasmonic waveguides.¹³ Several configurations of plasmon focusing in two-dimensions were demonstrated: by carefully organized particles on a surface,^{14,15} by spatial gratings,¹⁶ or by circular grooves within metal films,^{17,18} preferably excited by radially polarized light.^{19,20} This nanoconfinement leads to a local field enhancement, sufficient to improve nonlinearities,^{21,22} to increase a radiation efficiency of quantum

emitters,^{23,24} and to play a key role for nanolasers.^{25–27} Organized in ordered arrays or nanoclusters, plasmonic particles may serve as building blocks of artificial materials^{28,29} or efficient sensors,³⁰ while on-demand excitation of a nanosized particle by micrometer-sized optical wave is possible with careful engineering of an optical pulse.³¹

Here we demonstrate a plasmonic antenna that collects light from free space to be focused and captured in its near field, where an object of interest may be located. In our case another nanoantenna, a that which is a part of a transmitting antenna, is the object of interest. While a related configuration was recently examined theoretically in the context of near-field enhancement,³² here we perform scattering experiments (far-field measurements) to study the efficiency and coupling of resonances in the combined antenna struc-

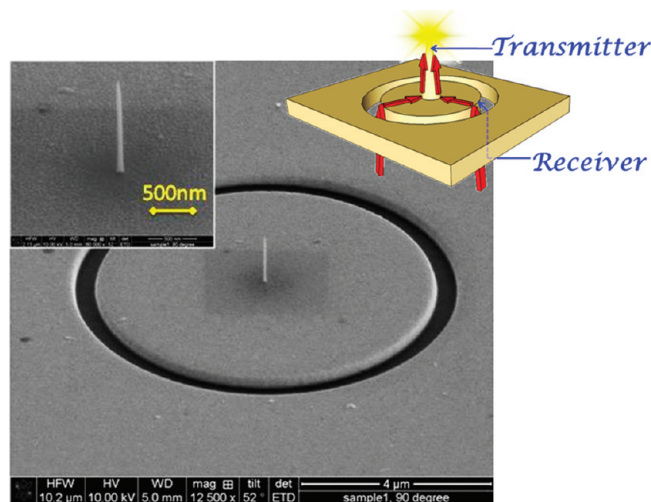


FIGURE 1. Experimental sample: plasmonic wire grown at the center of the etched circular slit. Right inset: scheme of coupled antennas action. Left inset: zoom on the antenna region.

* To whom correspondence should be addressed. E-mail: gpasha@tx.technion.ac.il.

Received for review: 10/12/2010

Published on Web: 12/06/2010

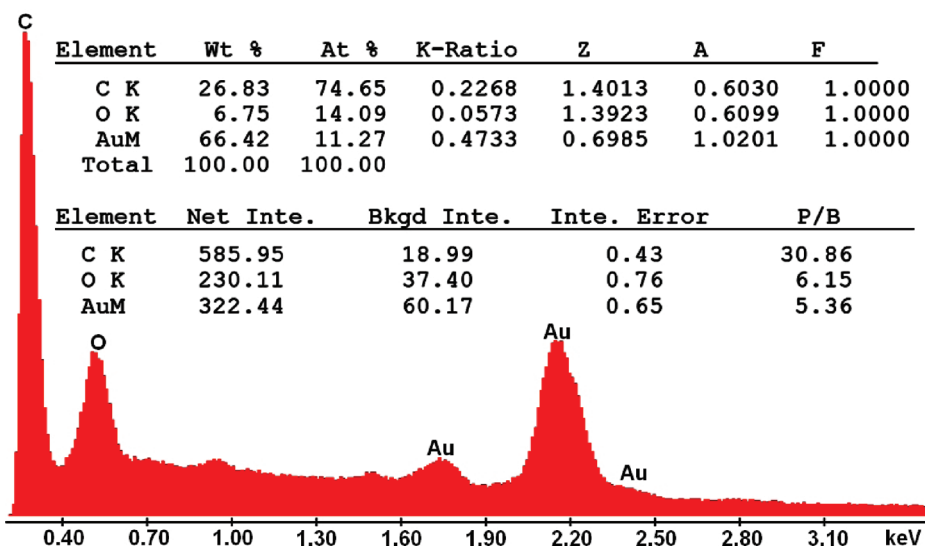


FIGURE 2. Material composition of the deposited wire, measured by EDX spectroscopy.

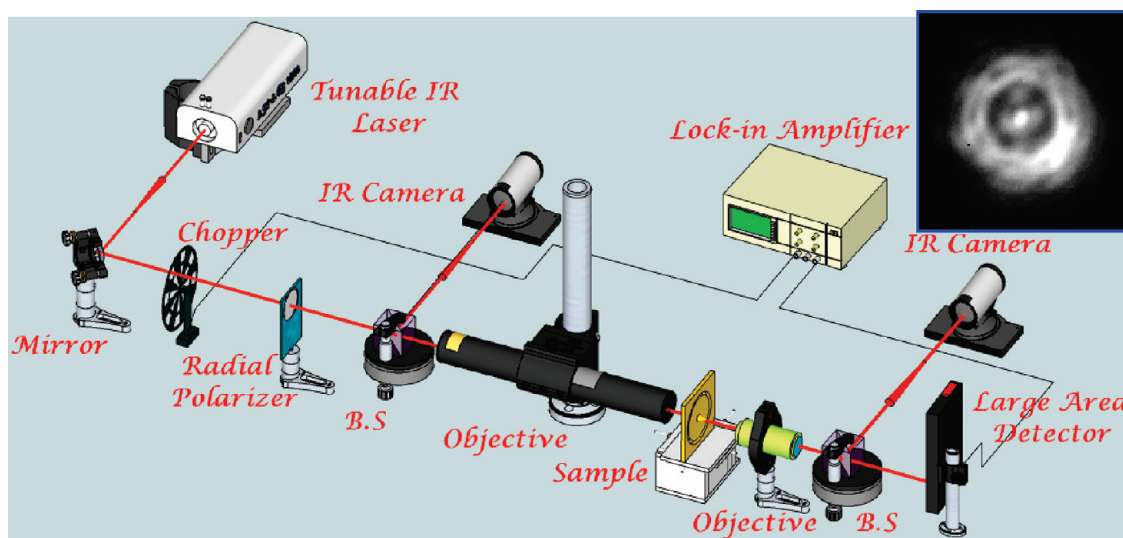


FIGURE 3. Measurement setup. A tunable NIR laser is radially polarized before impinging on the sample. Reflection path verifies “center of the beam on center of the sample” alignment. The transmitted light is collected and detected by a large-area InGaAs detector in a lock-in scheme. Inset: IR-camera image of “long” antenna sample focused at antenna plane.

ture. The structure is comprised of a receiving focusing plasmonic antenna (ring shaped), that converts the incoming beam to focused cylindrical plasmons on the rear side, which are subsequently coupled to a short vertical wire that assists in retransmitting to the far field (Figure 1).

The devices were fabricated by a two-step process at the same chamber. First, the circular ring was etched using focused ion beam (FIB) with a precise control over its dimensions. Subsequently, gold wires of different sizes were grown on the center of the ring by means of low current electron beam-assisted local deposition of Au from gas phase precursor. The deposition of Au by this process always results in some carbon contamination (usually substantial) that modifies the optical property of the Au wire, mainly reducing its high negative dielectric constant. Thus an energy-dispersive X-ray spectroscopy (EDX) was performed

to the Au wire, (Figure 2) confirming that a large percentage of carbon is diluting the deposited Au wire. These quantitative results were used to predict the actual permittivity of the wire.

Transmission spectra of the samples were measured using a tunable NIR laser (1510–1630 nm) having a radial polarization (radial polarizer was implemented by subwavelength grating on silicon). The radially polarized light was focused by a microscope objective on the center of the plasmonic receiving annular antenna via the glass substrate (verified by reflection path, Figure 3) and was collected on the output port by another high numerical aperture objective. The input light was chopped and the output was detected by a large-area InGaAs detector, engaged in a lock-in scheme (Figure 3). The IR-camera image taken from the

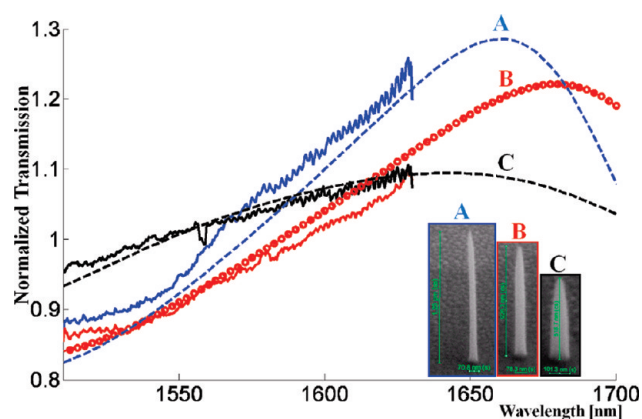


FIGURE 4. Transmission enhancement of the samples with wires, transmitter side in air, normalized by the ring antenna transmission. Measurement and theoretical fit of the following: long wire, solid blue line and dashed blue line; medium wire, solid red and red circles; and short wire, solid black and dashed-dotted black.

focusing on the antenna plane is presented in the figure inset, exhibiting the hotspot in the center.

The first set of experiments was performed when the plasmonic wire is embedded in air. The spectral transmission results are depicted in Figure 4. The transmission spectrum for the same receiving configuration and varying wire antenna dimensions was normalized by the spectral transmission of the ring antenna, which assisted also in elimination of the spectral response of the measurement system. The most significant signature in the transmission spectrum was recorded for the longest antenna, showing $\sim 30\%$ enhancement, indicating 3 orders of magnitude enhancement of the wire antenna cross section, estimated by the ratio of geometrical dimensions of the receiver ring and the wire as a stand-alone antenna. This effective cross section enhancement is of the same order of magnitude as for rigorously calculated “particle above a surface” structures³³ and exceeds significantly experimental results reported on single particles.³⁴ Since the resonance of the wire should be dependent on the embedding media, a second set of similar experiments were performed with the same devices after embedding the wire (the transmission region) in polyamide. The transmission peaks were blue shifted (Figure 5) (as predicted by simulations) and similar values of $\sim 30\%$ peak transmission enhancement were observed.

The finite element method (FEM) was used to comprehend the measured data and to fit it with the theoretical predictions. Circular symmetry of the structure was exploited for reduction of the computation complexity, allowing denser grid and enhanced accuracy. The dielectric property of the antennas was adjusted according to the dilution values of the Au by carbon as extracted from the X-rays spectroscopic data and by employing the effective index model. The best fit was achieved for $\epsilon \sim -18 + 2j$. Total transmitted power was evaluated by integration of the far field power over the relevant boundaries and presented as a function of the wavelength. The normalization was

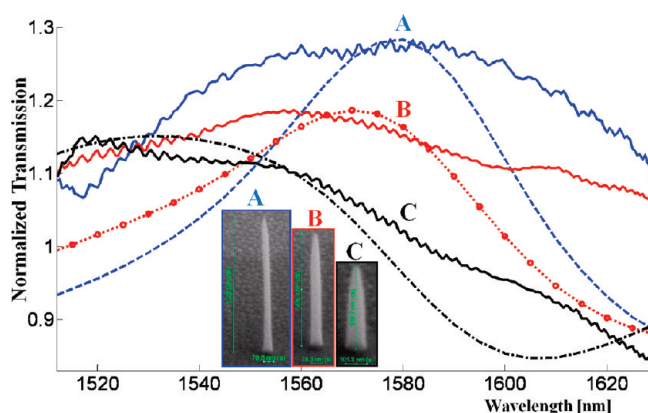


FIGURE 5. Transmission enhancement of the samples with wires, transmitter side covered by polyamide, normalized by the ring antenna transmission. Measurement and theoretical fit of the following: long wire, solid blue line and dashed blue line; medium wire, solid red and red circles; short wire, solid black and dashed-dotted black.

performed as it was done for the experimental data. A good fit to all sets of measurements was obtained by the model. The spectral peaks for the dielectrically embedded wire antenna, although located at the same wavelengths as recorded in the experiments, are narrower for the simulation, probably due to polymer layer. Polyamide, exhibited by stress induced striations, which are close enough to the metal tip to cause loss to the Fabry–Perot resonator, results in the broadening. Simulations, approximating this phenomenon to the first order by replacing the random scattering loss of the polyamide surface by distributed homogeneous loss of this layer ($\sim 1\%$ loss), verify this hypothesis. The transmission peaks correspond to the first Fabry–Perot resonances of the plasmonic wire antenna³⁵ that were recently calculated in ref 32.

A third set of experiments was performed to emphasize the unique role of the wire as part of the transmitting

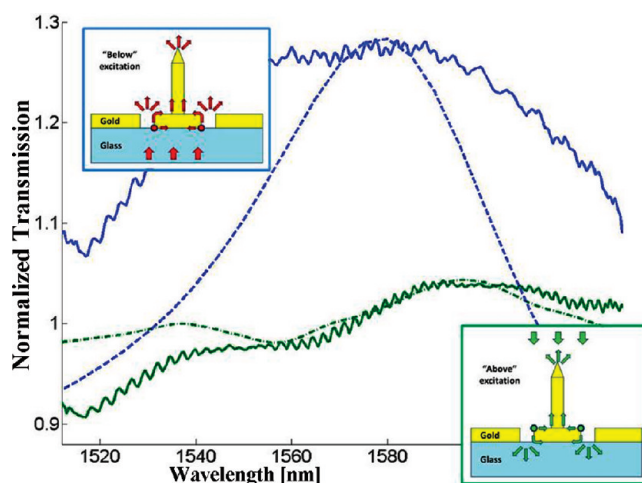


FIGURE 6. Transmission enhancement of the long wire sample of Figure 5. Measurement (solid) and theoretical fit (dashed) of excited from the receiving side “below” (as in Figure 5) and (green line) excited from transmitting side “above”. Insets: schemes of below and above scenarios.

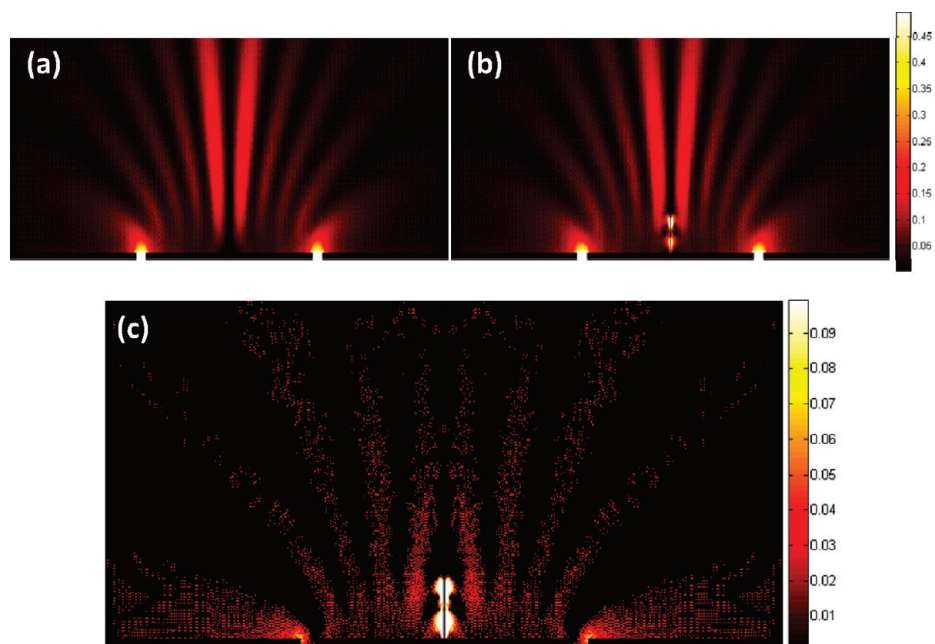


FIGURE 7. FEM simulation of power flow for the sample with the long wire of Figure 5 at the wire resonance wavelength of 1580 nm. (a) Annular receiving transmitting antennas, (b) adding the central wire, (c) distribution of the power difference.

antenna. When the excitation direction was flipped, the wire antenna became a part of the receiving antenna, which is contrary to the previous experiments. The normalized transmission was measured again and compared to the previous results (of polyamide-covered samples) in Figure 6, showing that when the wire is engaged within the receiving focusing antenna its contribution to the reception is minimal. This nonsymmetrical operation may be explained by the following: the regular excitation (top-left inset of Figure 6) creates SPP within the circular slit, which were efficiently converted to rear-side in-plane surface waves by a 90° coupling. These SPPs converge to the center¹⁸ and excite the wire. On resonance, the wire is becoming an effective secondary source which reemits diverging plasmonic waves; the latter are partially radiated from the annular slit, thus contributing additional portion from the near field to the far field. It can be seen from the power distributions and their difference plots in Figure 7 that the extra power is not radiated directly from the wire, but rather from the ring, preserving the same radiation pattern but with enhanced efficiency. On the other hand, in the flipped excitation (bottom-right inset of Figure 6), the wire antenna in the center of the input donut-shaped radially polarized beam has an insignificant interaction with the impinging field, thus not changing the transmittance of the ring shape antenna. This nonsymmetrical operation is actually not related to formal nonreciprocal operation; if the scattered field is reversed in time the exciting field is expected to appear at the output (neglecting the systems' loss). However, for many practical applications this nonsymmetrical operation is interesting by itself; in plasmonics, a number of devices with unidirectional operation were

demonstrated,^{36,37} including emission unidirectionality³⁸ and dielectric systems with gain.³⁹

In conclusion, we showed the response of a tandem plasmonic nanoantenna assembly by measurements of the far field spectral response of the coupled structure. Although having a very small nominal aperture, the plasmonic wire has a significant signature and enhancement in the far field, which amounts to almost 3 orders of magnitude of cross-section enhancement. The results are in good agreement with FEM numerical experiment with a reduced value of Au permittivity due to carbon dilution. The tandem approach may be very useful for excitation by a macroscopic beam of a single nanoantenna which is a challenging task. Commonly, arrays of antennas are used to increase overall scattering cross-section. Moreover, since the receiver dimensions do not have to be directly related to the excitation wavelength, the tandem may in principle be relatively small. All the above advantages may bring this concept to be very useful for biosensing, nonlinear elements, optical isolators, metamaterials building blocks, nanolithography, optically assisted magnetic memories, more efficient collection and transmission mode NSOM, and apertureless near-field instruments.

REFERENCES AND NOTES

- (1) Boltasseva, A.; Shalaev, V. M. Fabrication of optical negative-index metamaterials: recent advances and outlook, *Metamaterials (Amst.)* **2008**, *2* (1), 1–17.
- (2) Gramotnev, D. K.; Bozhevolnyi, S. I. Plasmonics beyond the diffraction limit. *Nat. Photonics* **2010**, *4*, 83–91.
- (3) Zayats, A. V.; Smolyaninov, I. I.; Maradudin, A. A. Nano-optics of surface plasmon polaritons. *Phys. Rep.* **2005**, *408* (3–4), 131–314.

- (4) Maier, A. *Plasmonics: Fundamentals and Applications*: Springer Science + Business Media LLC: New York, 2007.
- (5) Berini, P. Plasmon-polariton waves guided by thin lossy metal films of finite width: bound modes of symmetric structures. *Phys. Rev. B* **2000**, *61* (15), 10484–10503.
- (6) Prodan, E.; Radloff, C.; Halas, N. J.; Nordlander, P. A hybridization model for the plasmon response of complex nanostructures. *Science* **2003**, *302* (5644), 419–422.
- (7) Muhschlegel, P.; Eisler, H. J.; Martin, O. J. F.; Hecht, B.; Pohl, D. W. Resonant Optical Antennas. *Science* **2005**, *308*, 1607.
- (8) Rechberger, W.; Hohenau, A.; Leitner, A.; Krenn, J. R.; Lamprecht, B.; Aussenegg, F. R. Optical properties of two interacting gold nanoparticles. *Opt. Commun.* **2003**, *220*, 137–141.
- (9) Stockman, M. I. Nanofocusing of Optical Energy in Tapered Plasmonic Waveguides. *Phys. Rev. Lett.* **2004**, *93*, 137404.
- (10) Verhagen, E.; Spasenovic, M.; Polman, A.; Kuipers, L. (K.). Nanowire Plasmon Excitation by Adiabatic Mode Transformation. *Phys. Rev. Lett.* **2009**, *102*, 205904.
- (11) Ropers, C.; Neacsu, C. C.; Elsaesser, T.; Albrecht, M.; Raschke, M. B.; Lienau, C. Grating-Coupling of Surface Plasmons onto Metallic Tips: A Nanoconfined Light Source. *Nano Lett.* **2007**, *7* (9), 2784–2788.
- (12) Ginzburg, P.; Arbel, D.; Orenstein, M. Gap plasmon polariton structure for very efficient microscale-tonanoscale interfacing. *Opt. Lett.* **2006**, *31* (22), 3288–3290.
- (13) Ginzburg, P.; Orenstein, M. Plasmonic transmission lines: from micro to nano scale with $\lambda/4$ impedance matching. *Opt. Express* **2007**, *15* (11), 6762–6767.
- (14) Yin, L.; Vlasko-Vlasov, V. K.; Pearson, J.; Hiller, J. M.; Hua, J.; Welp, U.; Brown, D. E.; Kimball, C. W. Subwavelength focusing and guiding of surface plasmons. *Nano Lett.* **2005**, *5*, 1399–1402.
- (15) Radko, I. P.; Bozhevolnyi, S. I.; Evlyukhin, A. B.; Boltasseva, A. Surface plasmon polariton beam focusing with parabolic nanoparticle chains. *Opt. Express* **2007**, *15*, 6576–6582.
- (16) Lezec, H. J.; Degiron, A.; Devaux, E.; Linke, R. A.; Martin-Moreno, L.; Garcia-Vidal, F. J.; Ebbesen, T. W. Beaming light from a subwavelength aperture. *Science* **2002**, *297* (5582), 820–822.
- (17) Liu, Z.; Steele, J. M.; Srituravanich, W.; Pikus, Y.; Sun, C.; Zhang, X. Focusing surface plasmons with a plasmonic lens. *Nano Lett.* **2005**, *5* (9), 1726–1729.
- (18) Lerman, G. M.; Yanai, A.; Levy, U. Demonstration of nanofocusing by the use of plasmonic lens illuminated with radially polarized light. *Nano Lett.* **2009**, *9* (5), 2139–2143.
- (19) Yanai, A.; Levy, U. Plasmonic focusing with a coaxial structure illuminated by radially polarized light. *Opt. Express* **2009**, *17* (2), 924–932.
- (20) Chen, W.; Abeysinghe, D. C.; Nelson, R. L.; Zhan, Q. Plasmonic lens made of multiple concentric metallic rings under radially polarized illumination. *Nano Lett.* **2009**, *9* (12), 4320–4325.
- (21) Wurtz, G. A.; Zayats, A. V. Nonlinear surface plasmon polariton crystals. *Laser Photon. Rev.* **2008**, *2* (3), 125–135.
- (22) Ginzburg, P.; Hayat, A.; Berkovitch, N.; Orenstein, M. Nonlocal ponderomotive nonlinearity in plasmonics. *Opt. Lett.* **2010**, *35* (10), 1551–1553.
- (23) Khurgin, J. B.; Sun, G.; Soref, R. A. Enhancement of luminescence efficiency using surface plasmon polaritons: figures of merit. *J. Opt. Soc. Am. B* **2007**, *24* (8), 1968–1980.
- (24) Nevet, A.; Berkovitch, N.; Hayat, A.; Ginzburg, P.; Ginzach, S.; Sorias, O.; Orenstein, M. Plasmonic nanoantennas for broad-band enhancement of two-photon emission from semiconductors. *Nano Lett.* **2010**, *10*, 1848–1852.
- (25) Hill, M. T.; Oei, Y.; Smalbrugge, B.; Zhu, Y.; de Vries, T.; van Veldhoven, P. J.; van Otten, F. W. M.; Eijkemans, T. J.; Turkiewicz, J. P.; de Waardt, H.; Geluk, E.; Kwon, S.; Lee, Y.; Nötzel, R.; Smit, M. K. Lasing in metallic-coated nanocavities. *Nat. Photonics* **2007**, *1*, 589–594.
- (26) Nezhad, M. P.; Simic, A.; Bondarenko, O.; Slutsky, B.; Mizrahi, A.; Feng, L.; Lomakin, V.; Fainman, Y. Room-temperature sub-wavelength metallo-dielectric lasers. *Nat. Photonics* **2010**, *4*, 395–399.
- (27) Oulton, R. F.; Sorger, V. J.; Zentgraf, T.; Ma, R.; Gladden, C.; Dai, L.; Bartal, G.; Zhang, X. Plasmon lasers at deep subwavelength scale. *Nature* **2009**, *461*, 629.
- (28) Ziolkowski, R. W.; Engheta, N. *Metamaterials: Physics and Engineering Explorations*; IEEE Press, John Wiley & Sons, Inc.: New York, 2006.
- (29) Pollard, R. J.; Murphy, A.; Hendren, W. R.; Evans, P. R.; Atkinson, R.; Wurtz, G. A.; Zayats, A. V.; Podolskiy, V. A. Optical nonlocalities and additional waves in epsilon-near-zero metamaterials. *Phys. Rev. Lett.* **2009**, *102* (12), 127405.
- (30) Lassiter, J. B.; Sobhani, H.; Fan, J. A.; Kundu, J.; Capass, F.; Nordlander, P.; Halas, N. J. Fano Resonances in Plasmonic Nanoclusters: Geometrical and Chemical Tunability. *Nano Lett.* **2010**, *10*, 3184–3189.
- (31) Durach, M.; Rusina, A.; Nelson, K.; Stockman, M. I. Toward Full Spatio-Temporal Control on the Nanoscale. *Nano Lett.* **2007**, *7*, 3145–3149.
- (32) Normatov, A.; Ginzburg, P.; Berkovitch, N.; Lerman, G. M.; Yanai, A.; Levy, U.; Orenstein, M. Efficient coupling and field enhancement for the nano-scale: plasmonic needle. *Opt. Express* **2010**, *18*, 14079–14086.
- (33) Søndergaard, T.; Bozhevolnyi, S. I. Surface plasmon polariton scattering by a small particle placed near a metal surface: An analytical study. *Phys. Rev. B* **2004**, *69*, No. 045422.
- (34) Gunnarsson, L.; Rindzevicius, T.; Prikulis, J.; Kasemo, B.; Käll, M.; Zou, S.; Schatz, G. C. Confined Plasmons in Nanofabricated Single Silver Particle Pairs: Experimental Observations of Strong Interparticle Interactions. *J. Phys. Chem. B* **2005**, *109* (3), 1079–1087.
- (35) Ditlbacher, H.; Hohenau, A.; Wagner, D.; Kreibitz, U.; Rogers, M.; Hofer, F.; Aussenegg, F. R.; Krenn, J. R. Silver Nanowires as Surface Plasmon Resonators. *Phys. Rev. Lett.* **2005**, *95*, 257403.
- (36) López-Tejiera, F.; Rodrigo, S. G.; Martín-Moreno, L.; García-Vidal, F. J.; Devaux, E.; Ebbesen, T. W.; Krenn, J. R.; Radko, I. P.; Bozhevolnyi, S. I.; González, M. U.; Weeber, J. C.; Dereux, A. Efficient unidirectional nanoslit couplers for surface plasmons. *Nat. Phys.* **2007**, *3*, 324–328.
- (37) Dickson, R. M.; Lyon, L. A. Unidirectional Plasmon Propagation in Metallic Nanowires. *J. Phys. Chem. B* **2000**, *104*, 6095.
- (38) Curto, A. G.; Volpe, G.; Tamini, T. H.; Kreuzer, M. P.; Quidant, R.; van Hulst, N. F. Unidirectional Emission of a Quantum Dot Coupled to a Nanoantenna. *Science* **2010**, *329*, 930.
- (39) Ginzburg, P.; Hayat, A.; Vishnyakov, V.; Orenstein, M. Photonic logic by linear unidirectional interference. *Opt. Express* **2009**, *17*, 4251–4256.